AIAA JOURNAL
Vol. 35, No. 9, September 1997

Closed-Form Modeling of Fluid–Structure Interaction with Nonlinear Sloshing: Potential Flow

José L. Ortiz* and Alan A. Barhorst†
Texas Tech University, Lubbock, Texas 79409-1021

Closed-form modeling of the dynamics of a structure coupled to a rigid container carrying a fluid with a free surface is addressed. The coupling of the fluid's equations of motion with the structure's equations of motion is accomplished by building a boundary-value problem for the instantaneous interaction pressure. All nonlinearities are taken into account, and large-displacement nonlinear sloshing effects are considered; no simplifications are made in field equations and boundary conditions. This is a complementary study to a previous work presented by the authors. The boundary conditions for the interaction pressure when the container has curved walls are developed. The fluid is modeled as potential flow with modified Rayleigh damping. The end result of the analysis is a set of first-order differential equations for the motion of both the structure and the fluid. Numerical examples with circular containers are presented.

I. Introduction

To date, modeling nonlinear fluid sloshing in partially filled containers that are coupled to large-displacement structures has been treated approximately. Large amounts of the work deal with prescribed motion of the container, linearizations of the sloshing effects, or other simplifications. In this respect, finite differences,[1–6] finite elements,[7–10] and boundary element methods (BEM)[11–26] have been employed. Other simplified approaches can be found in Refs. 27–31. Also see Refs. 32–34 and the approximate approach in Ref. 35.

The main problem of coupling the equations of motion of a fluid with the equations of motion of a rigid container (coupled to a structure) is the complexity of the resulting set of equations. In this work, a closed-form coupling of both sets of equations is accomplished (without simplifications) by means of solving a pressure boundary-value problem for the instantaneous interaction pressure. Also, boundary conditions for the interaction pressure for the case of curved container walls are presented.

All nonlinearities inherent in the dynamics of the structure are taken into account; material and geometric nonlinearities can be considered. The fluid may be modeled with the Navier–Stokes equations or as potential flow.[36] However, only the potential flow model with modified Rayleigh damping is addressed in this work. All nonlinearities due to boundary conditions or sloshing effects are considered.

The end result of this methodology is a set of first-order differential equations for the motion of both the structure and the fluid. Numerical examples (two-dimensional) for the case of rigid circular containers are presented. This work complements previous work by the authors; see Ref. 37 for a formulation using the incompressible Navier–Stokes equations and experimental results justifying the methodology.

The paper will proceed by providing the mathematical formulation of the method followed by numerical examples and conclusions.

II. Mathematical Model

A two-dimensional rigid circular container carrying a fluid (Fig. 1a) will be used as reference for the description of the methodology; the case of an arbitrarily shaped container can be built analogously. The derivations are also valid for the three-dimensional case. There are three steps involved in coupling the motion of the fluid and the structure[36,37]: 1) finding the equations of motion for the structure as functions of the pressure field (Fig. 1b), 2) building a field equation for the pressure (in the fluid domain) as a function of the accelerations of the moving frame attached to the container, and 3) coupling these two sets of equations, provided a numerical solution for the pressure has been found.

A. Equations of Motion for the Structure

No details are given in obtaining the equations of motion for the structure. These can be found by any suitable method. We assume the equations are written in terms of the minimum set of independent coordinates; therefore, no constraint equations are involved; the methods in Refs. 38 and 39 are recommended. The discretized set of equations of motion can be put in the following form[36,37]:

$$[M]_{n\times n}\{\dot{U}_s\}_{n\times 1} = \{J\}_{n\times 1} + [D]_{n\times 3}\begin{Bmatrix} F_x \\ F_y \\ M_z \end{Bmatrix}_{3\times 1} \tag{1}$$

$$\{\dot{Q}_s\}_{n\times 1} = [C]_{n\times n}\{U_s\}_{n\times 1} \tag{2}$$

where n is the number of independent generalized coordinates Q_s and speeds U_s. Matrices $[M]$ and $[C]$ are the mass and kinematic matrices. Vector $\{J\}$ involves forcing terms not caused by the pressure p, whereas F_x, F_y, and M_z are components caused by p. In the context of Ref. 38, matrix $[D]$ contains components of partial velocities. Equation (1) will be revisited when building the coupled equations for the fluid–structure system.

B. Boundary Value for the Interaction Pressure

Before building the boundary value for the interaction pressure, the velocity potential ϕ has to be determined.

1. Velocity Potential

The boundary-value problem is[36,40]

$$\nabla^2\phi = 0 \qquad \text{in} \qquad V_f \tag{3}$$

$$\phi = \text{known} \qquad \text{on} \qquad S_f \tag{4}$$

$$\frac{\partial\phi}{\partial n} = (\boldsymbol{U} + \boldsymbol{\Omega}\times\boldsymbol{s})\cdot\boldsymbol{n} \qquad \text{on} \qquad S_w \tag{5}$$

(see nomenclature in Fig. 2), where ϕ and the absolute velocity $\boldsymbol{V}$ of fluid particles are related by the expression $\boldsymbol{V} = \nabla\phi$. Vector $\boldsymbol{U}$ is the translational velocity, and $\boldsymbol{\Omega}$ is the angular velocity of the moving frame F attached to the container. Vector $\boldsymbol{s}$ is the position of the

Received March 18, 1997; accepted for publication June 4, 1997.

*Visiting Assistant Professor, Department of Mechanical Engineering. Member AIAA.

†Assistant Professor, Department of Mechanical Engineering. Member AIAA.

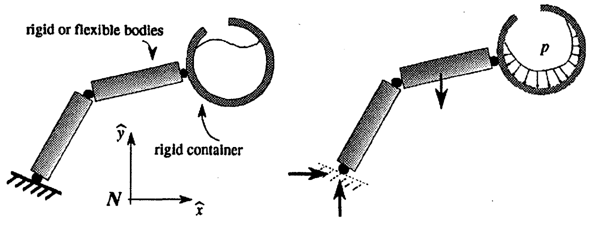

a) Problem statement **b) Structure free-body diagram**

Fig. 1 Fluid–structure system.

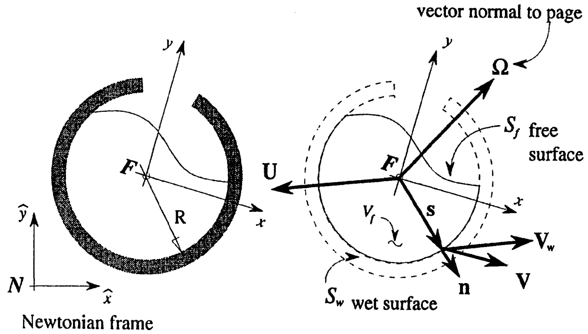

Fig. 2 Fluid nomenclature.

fluid particle as seen in the moving frame, and $\boldsymbol{n}$ is the normal to the surface. Using the BEM to solve for ϕ, the discrete equations are

$$[K]_{m\times m}\{\Phi\}_{m\times 1} = \{A\}_{m\times 1} \tag{6}$$

Array $\{\Phi\}$ stores both nodal values of the potential ϕ on the wet surface S_w and nodal values of the normal derivative of the potential on the free surface S_f. Velocities are found by numerical differentiation.

2. Field Equation for the Pressure

Starting with Euler's equation of motion with modified Rayleigh damping[41] and assuming constant body forces, the following field equation for the pressure is obtained:

$$\nabla^2 p = -\tfrac{1}{2}\rho\nabla^2(V^2) \quad \text{in} \quad V_f \tag{7}$$

where ρ is the density and V is the modulus of $\boldsymbol{V}$ (see details in Ref. 36).

3. Boundary Conditions for the Pressure

On the free surface S_f, the following dynamic boundary condition holds:

$$p = 0 \quad \text{on} \quad S_f \tag{8}$$

The pressure is arbitrarily set to zero without affecting the dynamics. Surface tension effects are not considered. On the wet surface S_w, the physical condition stating that fluid particles cannot pass through the walls results in the following kinematical condition:

$$\boldsymbol{u}\cdot\boldsymbol{n} = 0 \quad \text{on} \quad S_w \tag{9}$$

where $\boldsymbol{u}$ is the local velocity of the fluid particles (as seen in the moving frame F). Noticing that the components of both $\boldsymbol{u}$ and $\boldsymbol{n}$ are referred to the moving frame, differentiating Eq. (9) with respect to time results in

$$(\dot{\boldsymbol{u}} + \boldsymbol{\Omega}\times\boldsymbol{u})\cdot\boldsymbol{n} + \boldsymbol{u}\cdot(\boldsymbol{\Omega}'\times\boldsymbol{n}) = 0 \tag{10}$$

(Fig. 3), where $\boldsymbol{\Omega}'$ is the total angular velocity of frame G attached to a fluid particle. Frame G slides on a curved wall, as shown in Fig. 3. It can be shown that

$$\boldsymbol{\Omega}' = \boldsymbol{\Omega} + (u/R)\boldsymbol{k} \tag{11}$$

where u is the modulus of $\boldsymbol{u}$, R is the radius of curvature (arbitrarily taken as positive if the center of rotation is on the side of the fluid),

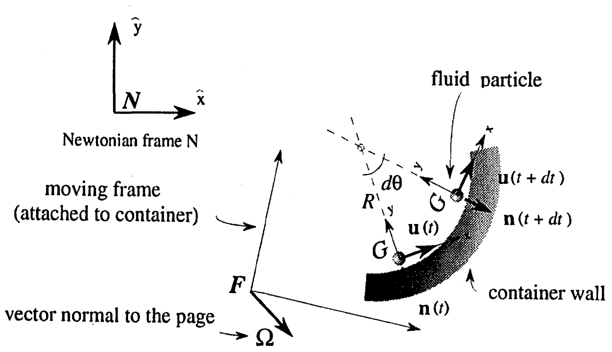

Fig. 3 Nomenclature for curved container walls.

and $\boldsymbol{k}$ is a unit vector normal to the page. After simplifications, Eq. (10) transforms to[36]

$$\dot{\boldsymbol{u}}\cdot\boldsymbol{n} = -(u^2/R) \quad \text{on} \quad S_w \tag{12}$$

The term $\dot{\boldsymbol{u}}$ appearing in Eq. (12) is the total acceleration (local plus convective) of fluid particles as measured in the moving frame F. Equation (12) has to be combined with the equation of motion of the fluid to obtain a boundary condition for the pressure. Euler's equation of motion with modified Rayleigh damping is[36,37]

$$\rho\dot{\boldsymbol{V}} = -\nabla p + \rho\boldsymbol{f} - \rho\mu\boldsymbol{u} \tag{13}$$

where $\boldsymbol{f}$ is the body force per unit mass, μ is a Rayleigh damping coefficient, and $\dot{\boldsymbol{V}}$ is the absolute (local plus convective) acceleration of fluid particles. Equation (13) can be rewritten as

$$\begin{aligned}\rho[\dot{\boldsymbol{U}} + \dot{\boldsymbol{u}} + 2\boldsymbol{\Omega}\times\boldsymbol{u} + \boldsymbol{\alpha}\times\boldsymbol{s} + \boldsymbol{\Omega}\times(\boldsymbol{\Omega}\times\boldsymbol{s})]\\ = -\nabla p + \rho\boldsymbol{f} - \rho\mu\boldsymbol{u}\end{aligned} \tag{14}$$

where $\dot{\boldsymbol{U}}$ and $\boldsymbol{\alpha}$ are the translational and angular accelerations of the moving frame F, respectively. Combining Eqs. (12) and (14), the following equation is obtained:

$$\begin{aligned}\frac{\partial p}{\partial n} &= \rho[\boldsymbol{f} - \dot{\boldsymbol{U}} - 2\boldsymbol{\Omega}\times\boldsymbol{u} - \boldsymbol{\alpha}\times\boldsymbol{s} - \boldsymbol{\Omega}\times(\boldsymbol{\Omega}\times\boldsymbol{s})]\cdot\boldsymbol{n}\\ &\quad + \rho\frac{u^2}{R} \quad \text{on} \quad S_w\end{aligned} \tag{15}$$

Except for $\dot{\boldsymbol{U}}$ and $\boldsymbol{\alpha}$, all terms on the right-hand side are known. Notice that both $\dot{\boldsymbol{U}}$ and $\boldsymbol{\alpha}$ are linear functions of the $\dot{U}_s$ used for describing the configuration of the structure. Therefore, the boundary condition for the pressure on S_w can be rewritten as

$$\frac{\partial p}{\partial n} = b + [E]_{1\times n}\{\dot{U}_s\}_{n\times 1} \tag{16}$$

where b and the row matrix $[E]$ are functions of the Q_s, the U_s, the fluid properties, and the kinematics of the moving frame. As before, n is the number of generalized coordinates describing the structure.

4. Numerical Solution for the Pressure

The boundary-value problem for the instantaneous interaction pressure is given by Eqs. (7), (8), and (16). Observe the linear relationship between p and the $\dot{U}_s$. Using the BEM to solve for p, the discretized equations are

$$[K]_{m\times m}\{P\}_{m\times 1} = \{G\}_{m\times 1} + [B]_{m\times n}\{\dot{U}_s\}_{n\times 1} \tag{17}$$

where column matrix $\{P\}$ stores nodal values of the pressure (or its normal derivatives) on the fluid boundaries. Matrices $\{G\}$ and $[B]$ appear naturally in the discretization process. It can be shown that matrix $[K]$ in Eq. (17) is the same as matrix $[K]$ in Eq. (6), provided the same mesh of boundary elements is used for solving for ϕ and p. Reusing the earlier factorized matrix $[K]$ (assembled when solving for ϕ) and using a standard solver with $n+1$ load cases, Eq. (17) is solved for p (as function of the accelerations $\dot{U}_s$), yielding

$$\{P\}_{m\times 1} = \{P_0\}_{m\times 1} + [P_1]_{m\times n}\{\dot{U}_s\}_{n\times 1} \tag{18}$$

This expression can now be used to build the instantaneous interaction forces (as function of the accelerations of the system). See more details in Ref. 36 and a more efficient solution to the pressure equations in Ref. 41

C. Coupling the Equations for the Fluid–Structure System

The final step in building the equations of motion for the fluid–structure system involves coupling Eq. (18) with Eq. (1). F_x, F_y, and M_z in Eq. (1) are given by

$$(F_x, F_y) = \int_{S_w} p\boldsymbol{n}\,\mathrm{d}S \tag{19}$$

$$M_z = \boldsymbol{k} \cdot \int_{S_w} \boldsymbol{s} \times p\boldsymbol{n}\,\mathrm{d}S \tag{20}$$

Using the nodal values of the pressure [Eq. (18)], Eqs. (19) and (20) are evaluated numerically, yielding

$$\begin{Bmatrix} F_x \\ F_y \\ M_z \end{Bmatrix}_{3\times 1} = \{I\}_{3\times 1} + [H]_{3\times n}\{\dot{U}_s\}_{n\times 1} \tag{21}$$

Putting this last equation into Eq. (1) leads to

$$\begin{aligned}[M]_{n\times n}\{\dot{U}_s\}_{n\times 1} &= \{J\}_{n\times 1} + [D]_{n\times 3}\{I\}_{3\times 1} \\ &\quad + [D]_{n\times 3}[H]_{3\times n}\{\dot{U}_s\}_{n\times 1}\end{aligned} \tag{22}$$

and after rearranging, the following is obtained:

$$[M']_{n\times n}\{\dot{U}_s\}_{n\times 1} = \{J'\}_{n\times 1} \tag{23}$$

where the new terms are

$$[M']_{n\times n} = [M]_{n\times n} - [D]_{n\times 3}[H]_{3\times n} \tag{24}$$

$$\{J'\}_{n\times 1} = \{J\}_{n\times 1} + [D]_{n\times 3}\{I\}_{3\times 1} \tag{25}$$

Equations (2) and (23) are the resulting set of explicit equations of motion for the coupled system and can be used with an assortment of integration schemes. However, solving Eqs. (2) and (23) allows updating the configuration of the structure only. Expressions for updating the configuration of the fluid must be developed.

D. Updating the Configuration of the Fluid

1. Updating the Position of the Free Surface

The approach labeled method III in Ref. 42 was implemented for updating the position of the free surface. Accordingly, the local velocity of computational nodes $\boldsymbol{u}_{cn}$ is

$$\boldsymbol{u}_{cn} = K(s_p - s)\boldsymbol{t} + u_n\boldsymbol{n} \tag{26}$$

where K is a positive constant, s_p is a preferred position along the arc, s is the current position along the arc, and u_n is the normal component of the local velocity $\boldsymbol{u}$. Vectors $\boldsymbol{t}$ and $\boldsymbol{n}$ are the normal and tangent vectors on the free surface. The value of s_p was obtained with the equal-length-element criterion.[42] The corresponding absolute velocity of computational nodes $\boldsymbol{V}_{cn}$ is given by

$$\boldsymbol{V}_{cn} = \boldsymbol{u}_{cn} + \boldsymbol{U} + \Omega \times \boldsymbol{s} \tag{27}$$

This absolute velocity is necessary for updating the position of the free surface, as shown in the next section.

2. Updating the Value of ϕ on the Free Surface

In the most general case, the rate of change of the velocity potential of a computational node moving with absolute velocity $\boldsymbol{V}_{cn}$ is given by

$$\frac{\mathrm{D}\phi}{\mathrm{D}t} = \frac{\partial\phi}{\partial t} + \nabla\phi \cdot \boldsymbol{V}_{cn} \tag{28}$$

Deriving a Bernoulli's equation by integrating Eq. (13) and combining it with Eq. (28), the following is obtained:

$$\frac{\mathrm{D}\phi}{\mathrm{D}t} = -\frac{1}{2}|\nabla\phi|^2 + f_x\hat{x} + f_y\hat{y} - \mu L + \nabla\phi \cdot \boldsymbol{V}_{cn} \tag{29}$$

where f_x and f_y are the global components of $\boldsymbol{f}$, $\hat{x}$ and $\hat{y}$ are global components of the free-surface position, and L is a potential such that $\nabla L = \boldsymbol{u}$ (see derivations and a discussion on the use of potential L instead of ϕ in Ref. 36; see a discussion on obtaining initial values for ϕ on the free surface in Ref. 42).

E. Resume of Formulas

Letting $Y = (U_s, Q_s, \phi, x, y)^T$ be the configuration of the fluid–structure system, the explicit set of equations of motion for the coupled system is

$$\dot{Y} = F(Y) \tag{30}$$

where $\dot{Y}$ and $F(Y)$ are

$$\dot{Y} = \begin{pmatrix} \dot{U}_s \\ \dot{Q}_s \\ \dfrac{\mathrm{D}\phi}{\mathrm{D}t} \\ \dfrac{\mathrm{D}x}{\mathrm{D}t} \\ \dfrac{\mathrm{D}y}{\mathrm{D}t} \end{pmatrix}$$

$$F(Y) = \begin{pmatrix} [M']^{-1}\{J'\} \\ [C]\{U_s\} \\ -\frac{1}{2}|\nabla\phi|^2 + f_x\hat{x} + f_y\hat{y} - \mu L + \nabla\phi \cdot \boldsymbol{V}_{cn} \\ \boldsymbol{u}_{cn}\cdot\boldsymbol{i} \\ \boldsymbol{u}_{cn}\cdot\boldsymbol{j} \end{pmatrix} \tag{31}$$

where ϕ is the solution of the boundary-value problem:

$$\nabla^2\phi = 0 \quad \text{in} \quad V_f$$

$$\phi = \text{prescribed} \quad \text{on} \quad S_f$$

$$\frac{\partial\phi}{\partial n} = (\boldsymbol{U} + \boldsymbol{\Omega} \times \boldsymbol{s}) \cdot \boldsymbol{n} \quad \text{on} \quad S_w$$

Matrices $[M']$ and $[J']$ are built by solving for p:

$$\nabla^2 p = -\frac{1}{2}\rho\nabla^2(V^2) \quad \text{in} \quad V_f$$

$$p = 0 \quad \text{on} \quad S_f$$

$$\frac{\partial p}{\partial n} = b + [E]_{1\times n}\{\dot{U}_s\}_{n\times 1} \quad \text{on} \quad S_w$$

Vector $\boldsymbol{V}_{cn}$ is built with the selected $\boldsymbol{u}_{cn}$, and potential L is found as explained in Ref. 36.

III. Numerical Examples

Three examples are presented illustrating the broad applicability of the methodology. In all cases, the BEM was implemented for solving the velocity potential and the pressure. No details are given on the numerical implementation of the BEM equations (see Ref. 43 for general details and Ref. 16 for details on handling the singularity of the velocity potential at the points where the free surface touches the walls). The pressure solution also has a singularity at the corners where the free surface touches the walls. It is the experience of the authors that this singularity has no influence on the coupled equations of motion [matrices $[M']$ and $[J']$ in Eq. (23)]. The volume correction and smoothing techniques were implemented using polar coordinates as described in Ref. 42.

In all examples, a fourth-order Runge–Kutta method was employed to integrate the equations and constant K in Eq. (26) was taken equal to $1/h$, where h is the time step.

A. Spring–Damper–Mass System

Figure 4a shows the nomenclature for the first example. The radius of the container was $R = 0.5$ m, the density of the fluid was $\rho = 1000$ kg/m^3, and the container was 50% filled. The Rayleigh damping coefficient was taken as 5% of the critical value.[15] Body forces per unit mass were taken as $f = (0, -9.8)$ m/s^2. Two nondimensional parameters were identified:

$$\gamma_1 = M_f/M_c, \qquad \beta_1 = w_f/w_{cf} \tag{32}$$

where M_c is the mass of the container and M_f is the mass of the fluid. The linear frequency of the fluid w_f (Ref. 44) and the frequency of the equivalent rigid-cargo system w_{cf} are given by

$$w_f = 1.169\sqrt{\frac{g}{D}}, \qquad w_{cf} = \sqrt{\frac{K}{M_f + M_c}} \tag{33}$$

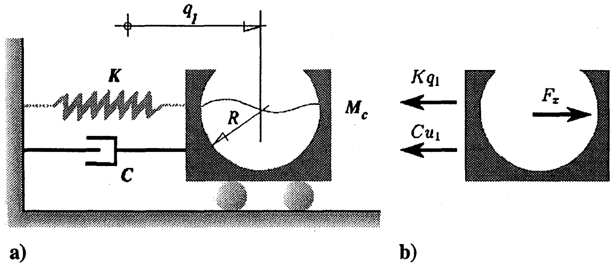

Fig. 4 Spring–damper–mass system.

where D is the container's diameter, g is the acceleration of gravity, and K is the spring constant. The equations of motion for the structure are

$$M_c\dot{u}_1 = -Cu_1 - Kq_1 + F_x \tag{34}$$

$$\dot{q}_1 = u_1 \tag{35}$$

(Fig. 4b), where C is taken equal to 5% of $2\sqrt{(KM_c)}$ and F_x is the interaction force due to the pressure. Solving for the ϕ and for p, the following is obtained [Eq. (18)]:

$$\{P\}_{m\times 1} = \{P_0\}_{m\times 1} + [P_1]_{m\times 1}\dot{u}_1 \tag{36}$$

which is employed in Eq. (19) to obtain

$$F_x = F_{x0} + F_{x1}\dot{u}_1 \tag{37}$$

Combining Eq. (34) with Eq. (37), the coupled equation of motion for the fluid–structure system is obtained [Eq. (23)]:

$$(M_c - F_{x1})\dot{u}_1 = -Cu_1 - Kq_1 + F_{x0} \tag{38}$$

Fixing the values of M_c, γ_1 and β_1, parameters M_f, w_{cf} and K can be calculated. Figure 5 shows the plots of the position of the container for the cases $M_c = 500$ kg, $\gamma_1 = 5.0$, and $\beta_1 = 0.5, 0.75, 1.0$, and 1.1. The plots also show the solutions for the corresponding equivalent rigid-cargo cases. As expected, for small values of γ_1 the responses of the system were close to the response of the equivalent

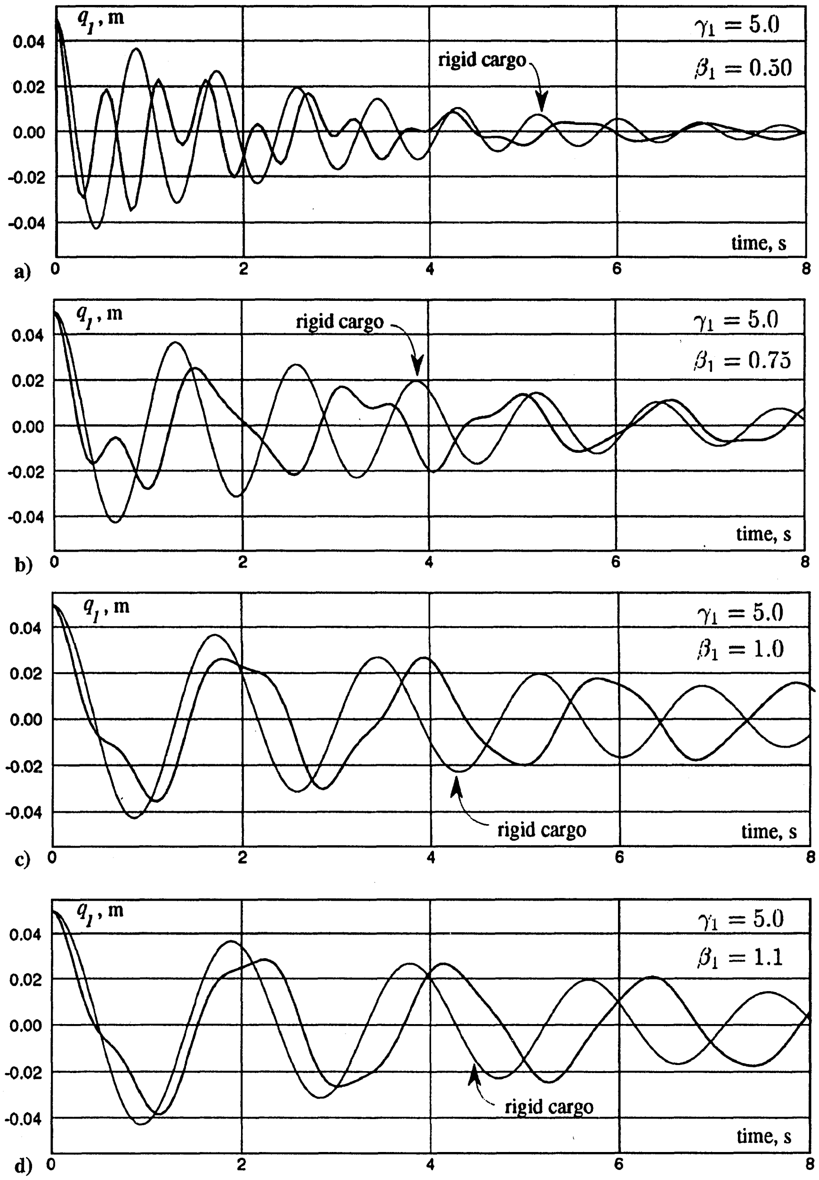

Fig. 5 Results for spring–damper–mass system.

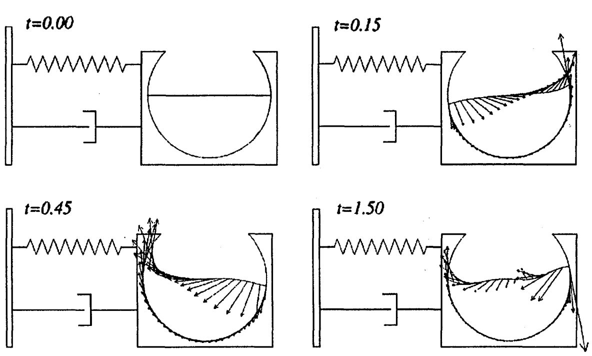

Fig. 6 Results for spring–damper–mass system.

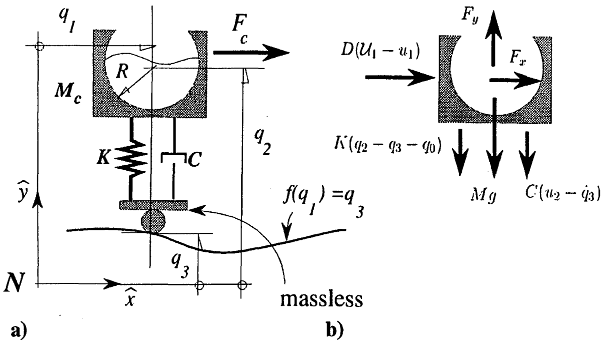

Fig. 7 Simple vehicle model.

rigid-cargo system (the structure drives the fluid), and they are not presented here. In all cases shown, the initial conditions were $q_1 = 0.05$ m and $u_1 = 0$. Figure 6 presents computer-generated plots showing the coupled system in motion for $\gamma_1 = 5.0$ and $\beta_1 = 0.5$ at selected times; also shown are the local velocity vectors. Although the motion of the fluid is highly nonlinear, the plot in Fig. 5a shows that the gross motion of the system resembles a two-degree-of-freedom system validating early approaches in which the fluid is modeled by an equivalent spring–mass system.[45] A similar study for a rectangular container can be found in Ref. 36.

B. Simple Vehicle Model

Figure 7a shows the nomenclature for a simple vehicle model. The radius of the container was $R = 0.5$ m, the density of the fluid was $\rho = 1000$ kg/m^3, body forces were $f = (0, -9.8)$ m/s^2, and the Rayleigh damping coefficient was taken 5% of the critical value. The container was 50% filled. For the structure, the spring constant was $K = 500{,}000$ N/m and C was 5% of the critical value $2\sqrt{(KM_c)}$, where M_c is the mass of the container. A simple control force $\boldsymbol{F}_c$ was modeled as

$$F_c = [D(\mathcal{U}_1 - u_1), 0] \tag{39}$$

where D is a given constant and $\mathcal{U}_1$ is a command velocity taken as $D = 60$ N · s/m and $\mathcal{U}_1 = 15$ m/s, respectively. The road was modeled as

$$q_3 = f(q_1) = A_1 \cos(w_1 q_1) + A_2 \cos(w_2 q_1) + S_1 q_1 \tag{40}$$

where $A_1 = 0.1$ m, $w_1 = 2\pi/40$ rad/m, $A_2 = 0.001$ m, $w_2 = 2\pi/5$ rad/m, and $S_1 = 0.002$. The equations of motion for the structure are

$$M_c \dot{u}_1 = D(\mathcal{U}_1 - u_1) + F_x \tag{41}$$

$$M_c \dot{u}_2 = -Mg - C(u_2 - \dot{q}_3) - K(q_2 - q_3 - q_0) + F_y \tag{42}$$

$$\dot{q}_1 = u_1 \tag{43}$$

$$\dot{q}_2 = u_2 \tag{44}$$

(Fig. 7b), where $q_0 = 0.51176$ m is the zero-force length for the spring, $\dot{q}_3 = f'(q_1)u_1$, and the interaction forces due to the fluid pressure are F_x and F_y. Solving for the interaction pressure as function of the accelerations [Eq. (18)] and integrating p [Eq. (19)], the following is obtained:

$$F_x = F_{x0} + F_{x1}\dot{u}_1 + F_{x2}\dot{u}_2 \tag{45}$$

$$F_y = F_{y0} + F_{y1}\dot{u}_1 + F_{y2}\dot{u}_2 \tag{46}$$

Combining these equations with the equations of motion for the structure, the equations for the coupled system are [Eq. (23)]

$$\begin{bmatrix} M_c - F_{x1} & -F_{x2} \\ -F_{y2} & M_c - F_{y2} \end{bmatrix} = \left\{ \begin{matrix} D(\mathcal{U}_1 - u_1) + F_{x0} \\ -Mg - C(u_2 - \dot{q}_3) - K(q_2 - q_3 - q_0) + F_{y0} \end{matrix} \right\} \tag{47}$$

Two cases were studied. In both cases, the total mass of the coupled system was kept equal to 600 kg by controlling the width of the container (perpendicular to the page). In case 1, the mass of the container was $M_c = 482.2$ kg and the width of the container (normal to the page) was set to $E = 0.3$ m to have a total mass of fluid $M_f = 117.8$ kg. In case 2, the mass of container and fluid were $M_c = 207.3$ kg and $M_f = 392.7$ kg, respectively. The mass ratios were

$$M_f / M_c = 0.24 \tag{48}$$

$$M_f / M_c = 1.89 \tag{49}$$

in cases 1 and 2, respectively. The limiting case of the rigid cargo (by setting $M_f = 0$) was also integrated for comparison. Figures 8a and 8b show the plots of q_2 and u_1 as function of time, respectively. Figure 8c shows plots of the free-surface position at the right wall. Figure 9 shows three computer-generated plots at selected times of the motion for case 1; the plots show the free-surface position and the local velocity vectors.

C. Robot Doing Maneuver

Figure 10 shows the nomenclature for the final example. This is a three-rigid-link robot with translational capability. The data for the fluid were $\rho = 1000$ kg/m^3, $f = (0, -9.8)$ m/s^2, and the Rayleigh damping coefficient was taken 5% of the critical value. The radius of the container was $R = 0.3$ m, and the width normal to the page was $E = 0.5$ m. The container was 50% filled.

The masses were $M_1 = 60$ kg, $M_2 = 10$ kg, and $M_3 = 10$ kg (container without fluid). The inertias were $I_2 = 0.83$ kg · m^2 and $I_3 = 0.9$ kg · m^2. The length were $g_1 = 1.5$ m, $g_2 = 1.0$ m, and $g_3 = 0.5$ m. The centers of gravity of bodies 1 and 2 were at the center of the bodies, respectively. The center of gravity of body 3 was at the origin of frame F. The control forces were modeled as

$$F_1 = -D_1 u_1 - K_1(q_1 - \mathcal{Q}_1) \tag{50}$$

$$T_1 = -D_2 u_2 - K_2(q_2 - \mathcal{Q}_2) + C_2 \tag{51}$$

$$T_2 = -D_3 u_3 - K_3(q_3 - \mathcal{Q}_3) + C_3 \tag{52}$$

The damping and stiffness terms were $D_1 = 200$ N · s/m, $D_2 = 1200$ N · m · s/rad, $D_3 = 500$ N · m · s/rad, $K_1 = 100$ N/m, $K_2 = 600$ N · m/rad, and $K_3 = 200$ N · m/rad. The constant terms were $C_2 = 990$ N · m and $C_3 = 395$ N · m. The command positions were $\mathcal{Q}_1 = 3.0$ m, $\mathcal{Q}_2 = 0.5$ rad, and $\mathcal{Q}_3 = 0$ rad.

The equations of motion of the structure [Eq. (1)] and the coupled equations [Eq. (23)] were obtained using Mathematica and then pasted into the main code. The Kane and Levinson approach[38] was employed to obtain the equations of motion of the robot. Initial conditions were $q_1 = 0$ m, $q_2 = -1.2$ rad, $q_3 = 0$ rad, and zero initial velocities. The time step was $h = 0.0025$ s. The rigid-cargo case was also studied for comparison; in that case (assuming the fluid is rigid), we have $M_3 = 80.7$ kg and $I_3 = 2.49$ kg · m^2.

Figure 11 shows selected computer-generated plots of the robot's configuration at selected times. Figure 12 shows plots of q_1, q_2, and q_3 as functions of time; the results for the rigid-cargo case are also shown.

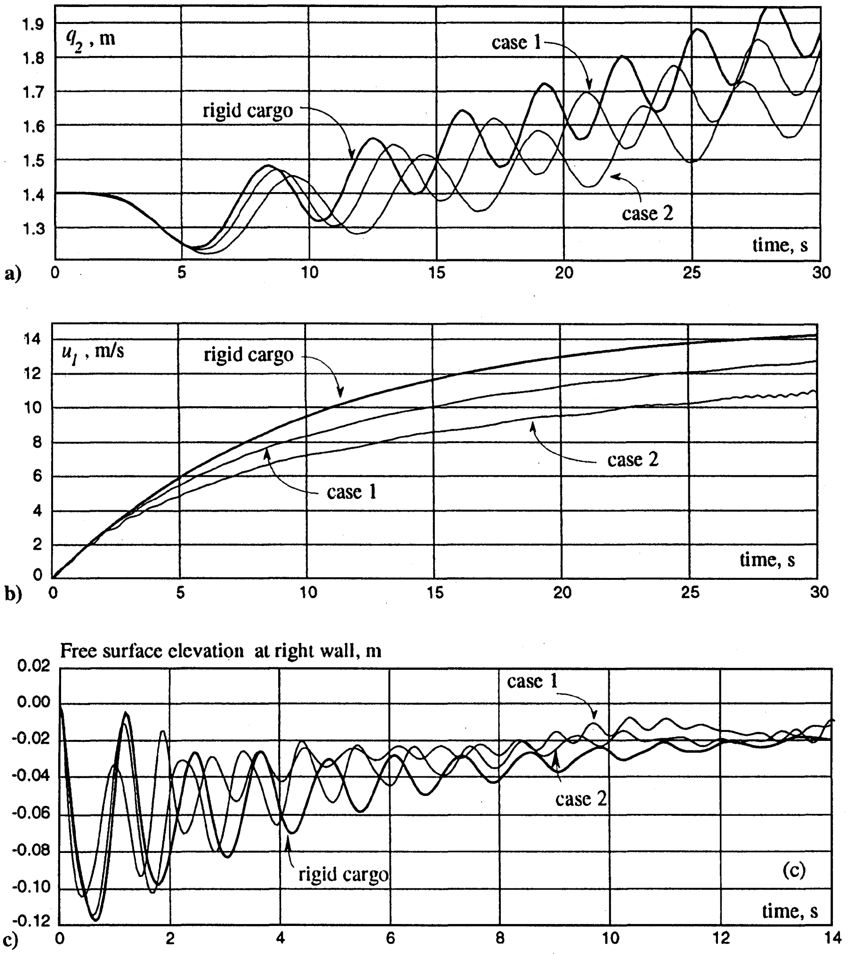

Fig. 8 Plots for a simple vehicle model.

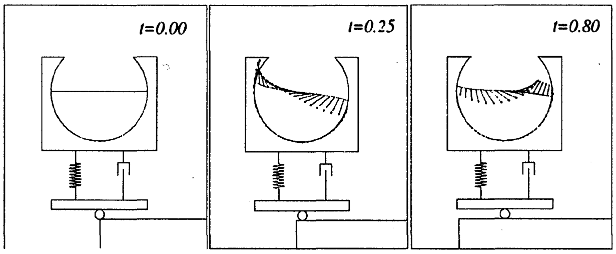

Fig. 9 Selected frames for a simple vehicle model, case 1.

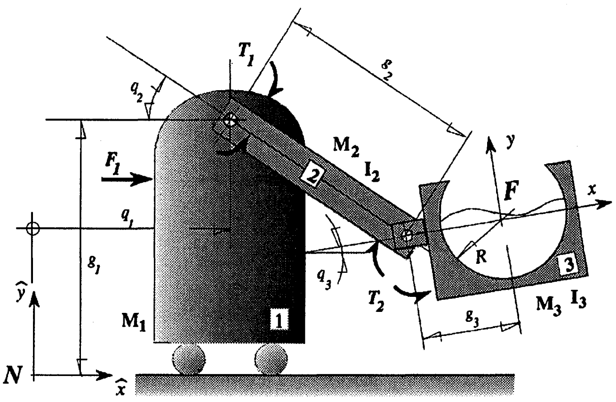

Fig. 10 Robot model.

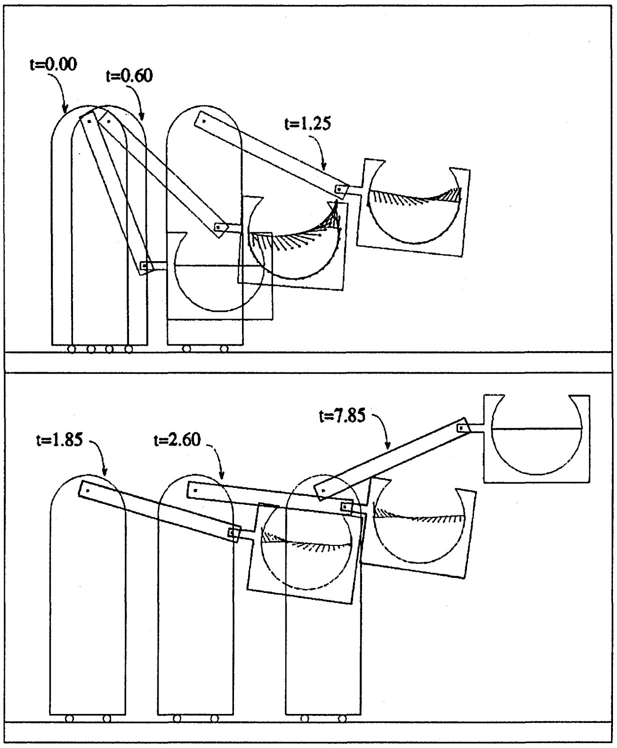

Fig. 11 Plots of robot model.

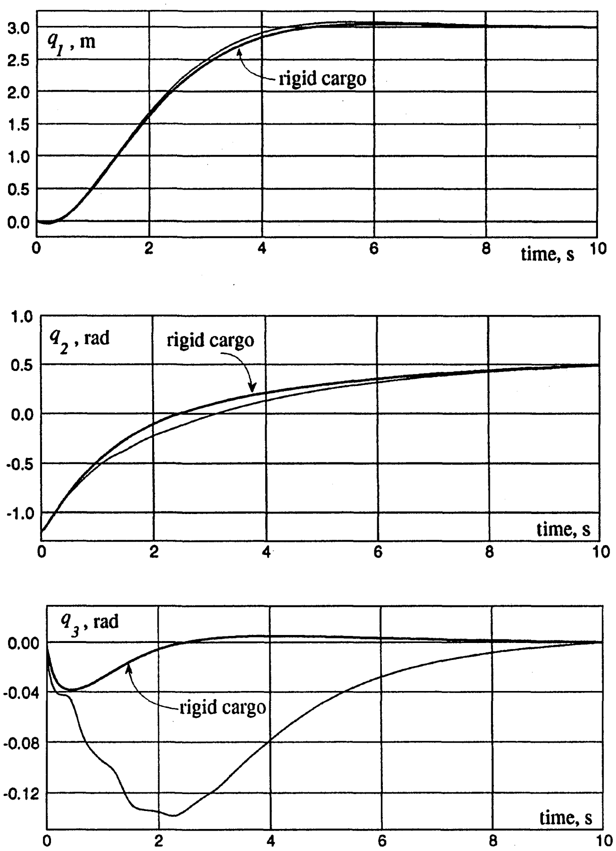

Fig. 12 Results of robot model.

IV. Conclusions

A method for modeling fluid–structure interaction problems has been presented. The coupling of equations was possible after building a boundary-value problem for the interaction pressure and observing the linearity of the pressure with respect to the accelerations of the moving frame attached to the fluid domain. This work complements previous work presented by the authors in which the case of the rectangular container was investigated. In this work, boundary conditions on the wet surface for the pressure problem, for curved container's walls, were derived.

The closed-form approach for coupling the equations of motion is general and has wide applicability. The incompressible Navier–Stokes equations with other numerical solutions techniques (such as finite differences) can be implemented.

References

[1]Chen, K.-H., and Pletcher, R. H., "Simulation of Three-Dimensional Liquid Sloshing Flows Using a Strongly Implicit Calculation Procedure," *AIAA Journal*, Vol. 31, No. 5, 1993, pp. 901–910.

[2]Hino, T., "Computation of a Free Surface Flow Around an Advancing Ship by the Navier–Stokes Equations," *Proceedings of the 5th International Conference on Numerical Ship Hydrodynamics* (Hiroshima, Japan), National Academy Press, Washington, DC, 1990, pp. 103–117.

[3]Hoekstra, M., "Recent Developments in a Ship Stern Flow Prediction Code," *Proceedings of the 5th International Conference on Numerical Ship Hydrodynamics* (Hiroshima, Japan), National Academy Press, Washington, DC, 1990, pp. 87–101.

[4]Miyata, H., Sato, T., and Baba, N., "Difference Solution of a Viscous Flow with Free-Surface Wave About an Advancing Ship," *Journal of Computational Physics*, Vol. 72, 1987, pp. 393–421.

[5]Popov, G., Sankar, S., Sankar, T. S., and Vatistas, G. H., "Liquid Sloshing in Rectangular Road Containers," *Computers and Fluids Journal*, Vol. 21, No. 4, 1992, pp. 551–569.

[6]Zhu, M., Miyata, H., and Kajitani, H., "Finite-Difference Simulation of a Viscous Flow About a Ship of Arbitrary Configuration," *Proceedings of the 5th International Conference on Numerical Ship Hydrodynamics* (Hiroshima, Japan), National Academy Press, Washington, DC, 1990, pp. 119–131.

[7]Agrawal, B. N., "Dynamic Characteristics of Liquid Motion in Partially Filled Tanks of a Spinning Spacecraft," *Journal of Guidance, Control, and Dynamics*, Vol. 16, No. 4, 1993, pp. 636–640.

[8]Bai, K. J., Kim, J. W., and Kim, Y. H., "Numerical Computations for a Nonlinear Free Surface Flow Problem," *Proceedings of the 5th International Conference on Numerical Ship Hydrodynamics* (Hiroshima, Japan), National Academy Press, Washington, DC, 1990, pp. 403–419.

[9]Nakayama, T., and Washizu, K., "Nonlinear Analysis of Liquid Motion in a Container Subjected to Forced Pitching Oscillation," *International Journal for Numerical Methods in Engineering*, Vol. 15, 1980, pp. 1207–1220.

[10]Ru-De, F., "Finite Element Analysis of Lateral Sloshing Response in Axisymmetric Tanks with Triangular Elements," *Computational Mechanics*, Vol. 12, 1993, pp. 51–58.

[11]Casciola, C. M., and Piva, R., "A Boundary Integral Formulation for Free Surface Viscous and Inviscid Flows About Submerged Bodies," *Proceedings of the 5th International Conference on Numerical Ship Hydrodynamics* (Hiroshima, Japan), National Academy Press, Washington, DC, 1990, pp. 469–479.

[12]Casciola, C. M., and Piva, R., "A Boundary Integral Approach in Primitive Variables for Free Surface Flows," *Proceedings of the 18th Symposium on Naval Hydrodynamics*, National Academy Press, Washington, DC, 1991, pp. 221–237.

[13]Cointe, R., Molin, B., and Nays, P., "Nonlinear and Second-Order Transient Waves in a Rectangular Tank," *BOSS'88: Proceedings of the International Conference on Behavior of Offshore Structures* (Trondheim, Norway), Tapir, Trondheim, Norway, 1988, pp. 705–718.

[14]Dommermuth, D. G., and Yue, D. K. P., "Numerical Simulations of Nonlinear Axisymmetric Flows with a Free Surface," *Journal of Fluid Mechanics*, Vol. 178, 1987, pp. 195–219.

[15]Faltinsen, O. M., "A Numerical Nonlinear Method of Sloshing in Tanks with Two-Dimensional Flow," *Journal of Ship Research*, Vol. 22, No. 3, 1978, pp. 193–202.

[16]Grilli, S. T., and Svendsen, I. A., "Corner Problems and Global Accuracy in the Boundary Element Solution of Nonlinear Wave Flows," *Engineering Analysis with Boundary Elements*, Vol. 7, No. 4, 1990, pp. 178–195.

[17]Hwang, J. H., Kim, I. S., Seol, Y. S., Lee, S. C., and Chon, Y. K., "Numerical Simulation of Liquid Sloshing in Three-Dimensional Tanks," *Computers and Structures*, Vol. 44, Nos. 1/2, 1992, pp. 339–342.

[18]Hwang, J. H., Kim, Y. J., and Kim, S. Y., "Nonlinear Hydrodynamic Forces Due to Two-Dimensional Forced Oscillation," *Nonlinear Water Waves IUTAM Symposium* (Tokyo, Japan), Springer–Verlag, Berlin, 1988, pp. 231–238.

[19]Lin, W.-M., Newman, J. N., and Yue, D. K., "Nonlinear Forced Motions of Floating Bodies," *Fifteenth Symposium Naval Hydrodynamics: Seakeeping Problems, Hull Propeller Interactions, Nonlinear Free-Surface Problems, Frontier Problems in Hydrodynamics*, National Academy Press, Washington, DC, 1985, pp. 33–49.

[20]Liu, P. L.-F., and Liggett, J. A., "Applications of Boundary Element Methods to Problems of Water Waves," *Developments in Boundary Element Methods*, Vol. 2, edited by P. K. Banerjee and R. P. Shaw, Applied Science, London, 1982, pp. 37–67.

[21]Liu, P. L.-F., and Liggett, J. A., "Boundary Element Formulations and Solutions for Some Non-Linear Water Wave Problems," *Developments in Boundary Element Methods*, Vol. 3, edited by P. K. Banerjee and R. P. Shaw, Applied Science, London, 1984, pp. 171–190.

[22]Nakayama, T., "Boundary Element Analysis of Nonlinear Water Wave Problems," *International Journal for Numerical Methods in Engineering*, Vol. 19, 1983, pp. 953–970.

[23]Nakayama, T., and Tanaka, H., "A Numerical Method for the Analysis of Nonlinear Sloshing in Circular Cylindrical Containers," *Boundary Integral Methods, Theory and Applications*, edited by L. Morino and R. Piva, Proceedings of the IABEM Symposium (Rome, Italy), Springer–Verlag, Berlin, 1991, pp. 359–368.

[24]Nakayama, T., and Washizu, K., "Boundary Element Analysis of Non-Linear Sloshing Problems," *Developments in Boundary Element Methods*, Vol. 3, edited by P. K. Banerjee and R. P. Shaw, Applied Science, London, 1984, pp. 191–211.

[25]Nestegard, A., and Sclavounos, P. D., "A Numerical Solution of Two-Dimensional Deep Water Wave-Body Problems," *Journal of Ship Research*, Vol. 28, No. 1, 1984, pp. 48–54.

[26]Romero, V. J., and Ingber, M. S., "A Numerical Model for 2-D Sloshing of Pseudo-Viscous Liquids in Horizontally Accelerated Rectangular Containers," *Boundary Elements XVII, Proceedings of the 17th International Conference on Boundary Elements* (Madison, WI), edited by C. A. Brebbia, Computational Mechanics Publications, Southampton, England, UK, 1995, pp. 567–583.

[27]Lui, A. P., and Lou, J. Y. K., "Dynamic Coupling of a Liquid-Tank System Under Transient Excitations," *Ocean Engineering*, Vol. 17, No. 3, 1990, pp. 263–277.

[28]Cointe, R., Geyer, P., King, B., Molin, B., and Tramoni, M., "Nonlinear and Linear Motions of a Rectangular Barge in a Perfect Fluid," *Proceedings of the 18th Symposium on Naval Hydrodynamics*, National Academy Press, Washington, DC, 1991, pp. 85–99.

[29]Falch, S., "Slamming of Flat-Bottomed Bodies Calculated with Exact Free Surface Boundary Conditions," *Proceedings of the 5th International Conference on Numerical Ship Hydrodynamics* (Hiroshima, Japan), National Academy Press, Washington, DC, 1990, pp. 251–267.

[30]Sen, D., Pawlowski, J. S., Lever, J., and Hinchey, M. J., "Two-Dimensional Numerical Modelling of Large Motions of Floating Bodies in Waves," *Proceedings of the 5th International Conference on Numerical Ship Hydrodynamics* (Hiroshima, Japan), National Academy Press, Washington, DC, 1990, pp. 351–373.

[31]Abramson, H. N., "The Dynamic Behavior of Liquids in Moving Containers with Applications to Space Vehicle Technology," NASA SP-106, 1966.

[32]Morand, H. J. P., and Ohayon, R., *Fluid Structure Interaction*, Wiley, Paris, 1995.

[33]Everstine, G. C., and Au-Yang, M. K. (eds.), *Advances in Fluid–Structure Interaction—1984*, American Society of Mechanical Engineers, New York, 1984.

[34]Crolet, J. M., and Ohayon, R. (eds.), *Computational Methods for Fluid–Structure Interaction*, Pitman Research Notes in Mathematics Series, Wiley, New York, 1994.

[35]Sankar, S., Ranganathan, R., and Rakheja, S., "Impact of Dynamics Fluid Slosh Loads on the Directional Response of Tank Vehicles," *Vehicle System Dynamics*, Vol. 21, 1992, pp. 385–404.

[36]Ortiz, J. L., "Modeling Flexible Multibody Systems-Fluid Interaction," Ph.D. Thesis, Dept. of Mechanical Engineering, Texas Tech Univ., Lubbock, TX, Dec. 1996.

[37]Ortiz, J. L., and Barhorst, A. A., "On Modeling Fluid–Structure Interaction," AIAA Paper 97-0785, Jan. 1997.

[38]Kane, T. R., and Levinson, D. A., *Dynamics: Theory and Applications*, McGraw–Hill, New York, 1985.

[39]Barhorst, A. A., and Everett, L. J., "Modeling Hybrid Parameter Multiple Body Systems: A Different Approach," *International Journal of Non-linear Mechanics*, Vol. 30, No. 1, 1995, pp. 1–21.

[40]Fletcher, C. A. J., *Computational Techniques for Fluid Dynamics*, 2nd ed. Vols. 1 and 2, Springer–Verlag, New York, 1991.

[41]Ortiz, J. L., Barhorst, A. A., and Robinett, R. D., "Flexible Multibody Systems–Fluid Interaction," *International Journal for Numerical Methods in Engineering* (to be published).

[42]Ortiz, J. L., and Barhorst, A. A., "Large-Displacement Nonlinear Sloshing in 2-D Circular Containers—Prescribed Motion of the Container," *International Journal for Numerical Methods in Engineering* (submitted for publication).

[43]Brebbia, C. A., Telles, J. C. F., and Wrobel, L. C., *Boundary Element Techniques, Theory and Applications in Engineering*, Springer–Verlag, New York, 1984.

[44]Lamb, H., *Hydrodynamics*, 6th ed., Dover, New York, 1945.

[45]Housner, G. W., "The Dynamic Behavior of Water Tanks," *Bulletin of the Seismological Society of America*, Vol. 53, No. 2, 1963, pp. 381–387.

J. Kallinderis
Associate Editor